

# Inverse Regulation of Rotation of $F_1$ -ATPase by the Mutation at the Regulatory Region on the $\gamma$ Subunit of Chloroplast ATP Synthase\*

Received for publication, January 20, 2004, and in revised form, January 26, 2004  
Published, JBC Papers in Press, January 26, 2004, DOI 10.1074/jbc.M400607200

Hanayo Ueoka-Nakanishi<sup>‡§</sup>, Yoichi Nakanishi<sup>‡¶</sup>, Hiroki Konno<sup>‡§</sup>, Ken Motohashi<sup>‡§</sup>,  
Dirk Bald<sup>||</sup>, and Toru Hisabori<sup>‡§\*\*</sup>

From the <sup>‡</sup>ATP System Project, Exploratory Research for Advanced Technology (ERATO), Japan Science and Technology Agency (JST), 5800-3 Nagatsuta-cho, Midori-ku, Yokohama 226-0026, Japan, <sup>§</sup>The Chemical Resources Laboratory, Tokyo Institute of Technology, Nagatsuta 4259, Midori-ku, Yokohama 226-8503, Japan, <sup>¶</sup>Laboratory of Cell Dynamics, Graduate School of Bioagricultural Sciences, Nagoya University, Nagoya 464-8601, Japan, and <sup>||</sup>Department of Structural Biology, Free University of Amsterdam, De Boelelaan 1087, 1081 Amsterdam, The Netherlands

In  $F_1$ -ATPase, the rotation of the central axis subunit  $\gamma$  relative to the surrounding  $\alpha_3\beta_3$  subunits is coupled to ATP hydrolysis. We previously reported that the introduced regulatory region of the  $\gamma$  subunit of chloroplast  $F_1$ -ATPase can modulate rotation of the  $\gamma$  subunit of the thermophilic bacterial  $F_1$ -ATPase (Bald, D., Noji, H., Yoshida, M., Hirono-Hara, Y., and Hisabori, T. (2001) *J. Biol. Chem.* 276, 39505–39507). The attenuated enzyme activity of this chimeric enzyme under oxidizing conditions was characterized by frequent and long pauses of rotation of  $\gamma$ . In this study, we report an inverse regulation of the  $\gamma$  subunit rotation in the newly engineered  $F_1$ -chimeric complex whose three negatively charged residues Glu<sup>210</sup>-Asp<sup>211</sup>-Glu<sup>212</sup> adjacent to two cysteine residues of the regulatory region derived from chloroplast  $F_1$ -ATPase  $\gamma$  were deleted. ATP hydrolysis activity of the mutant complex was stimulated up to 2-fold by the formation of the disulfide bond at the regulatory region by oxidation. We successfully observed inverse redox switching of rotation of  $\gamma$  using this mutant complex. The complex exhibited long and frequent pauses in its  $\gamma$  rotation when reduced, but the rotation rates between pauses remained unaltered. Hence, the suppression or activation of the redox-sensitive  $F_1$ -ATPase can be explained in terms of the change in the rotation behavior at a single molecule level. These results obtained by the single molecule analysis of the redox regulation provide further insights into the regulation mechanism of the rotary enzyme.

$F_0F_1$ -ATP synthase, which resides in the bacterial plasma membranes, mitochondrial inner membranes, and chloroplast thylakoid membranes, synthesizes ATP from ADP and inorganic phosphate using a proton gradient across the membranes as an energy source (1–3). The enzyme consists of two parts, a membrane-intrinsic  $F_0$  part responsible for proton translocation and a membrane-extrinsic  $F_1$  part, in which ATP is hydrolyzed or synthesized. The  $F_1$  part consists of  $\alpha_3\beta_3\gamma_1\delta_1\epsilon_1$  subunits (4), and the whole structure is very similar in all  $F_1$ . As the isolated  $F_1$  part catalyzes ATP hydrolysis, it is called  $F_1$ -

ATPase. The  $\alpha_3\beta_3\gamma$  subcomplex from  $F_1$  is the minimum core complex that maintains the feature of  $F_1$  as ATPase (5). The three-dimensional structure of the major part of bovine heart mitochondrial  $F_1$ -ATPase determined by the x-ray crystal analysis revealed an alternating hexagonal arrangement of three  $\alpha$  and three  $\beta$  subunits around the  $\gamma$  subunit, which is located in the central cavity (6). This remarkable finding strongly supported the idea of rotation of the  $\gamma$  subunit relative to the  $\alpha_3\beta_3$  hexagon, which had been first proposed by P. D. Boyer from the analysis of catalytic site cooperativity (7). In 1997, the actual rotation of the  $\gamma$  subunit coupled with ATP hydrolysis was directly visualized under an optical microscope by attaching a fluorescent-labeled actin filament to the  $\gamma$  subunit of the  $\alpha_3\beta_3\gamma$  subcomplex (8). Thereafter, rotation of the  $\gamma$  subunit was shown in *Escherichia coli*  $F_1$  (9, 10) and chloroplast  $F_1$  (11) using the same method.

The chloroplast ATP synthase ( $CF_0CF_1$ )<sup>1</sup> has fundamentally an identical structure to other  $F_0F_1$ -ATP synthases (12). However, the enzymatic activity of chloroplast ATP synthase from higher plants and green algae is highly regulated by several ways, such as activation by a proton gradient across the membranes (13), deactivation by a 14-3-3 protein (14), and activation by reduction of a disulfide bond on the  $\gamma$  subunit (15, 16). Especially, the redox dependent regulation of the enzyme activity is only observed on the chloroplast  $F_1$  ( $CF_1$ ). ATPase activity of the isolated  $CF_1$  is enhanced when the disulfide bond is cleaved by reduction. *In vivo*, this reduction is achieved by thioredoxin, which is a major reductant protein in chloroplasts, and is reduced by electrons supplied from the photosystem (17). The structural basis for this redox regulation is assigned to the special portion of the  $\gamma$  subunit, which consists of 37 amino acid residues (Pro<sup>194</sup>-Ile<sup>230</sup> in the case of spinach  $CF_1$ ) including two cysteine residues (Cys<sup>199</sup> and Cys<sup>205</sup> in spinach) (18). This portion resides only in the  $\gamma$  subunit of the redox-sensitive ATP synthase. In case of cyanobacteria, 9 amino acids including 2 critical cysteines are missing in the region and the enzyme is redox-insensitive. Introduction of these 9 amino acid residues

\* This work was supported by the ATP System Project, ERATO funded by the Japan Science and Technology Agency, and in part by the Grant-in-aid for Science Research 13440238 (to T. H.) from Japan Society for the Promotion of Science. The costs of publication of this article were defrayed in part by the payment of page charges. This article must therefore be hereby marked "advertisement" in accordance with 18 U.S.C. Section 1734 solely to indicate this fact.

\*\* To whom correspondence should be addressed. E-mail: thisabor@res.titech.ac.jp.

<sup>1</sup> The abbreviations used are:  $CF_0CF_1$ , ATP synthase from chloroplast thylakoid membrane;  $CF_1$ , chloroplast coupling factor 1;  $TF_1$ ,  $F_1$  subcomplex from plasma membranes of thermophilic bacterium *Bacillus PS3*; DTT, dithiothreitol; DTNB, 5,5'-dithiobis-(2-nitrobenzoic acid); AMS, 4-acetamido-4'-maleimidyl-stilbene-2,2'-disulfonate; BSA, bovine serum albumin; TCT,  $F_1$  chimeric complex composed of  $\alpha_3$ ,  $\beta_3$ , and  $\gamma$  in which 111 residues from Val<sup>92</sup> to Phe<sup>202</sup> was replaced by 148 residues of the counterpart from spinach  $CF_1$ - $\gamma$ ;  $\Delta EDE$ , altered TCT chimeric complex in which Glu<sup>210</sup>, Asp<sup>211</sup>, and Glu<sup>212</sup> were deleted from the chimeric  $\gamma$  subunit; biotin-PEAC5-maleimide, 6-[N'-(2-(N-maleimide)ethyl)-N-piperazinylamido]hexyl-D-bionamide; MOPS, 4-morpholinepropane-sulfonic acid.

from spinach  $CF_1$ - $\gamma$  into the cyanobacterial  $F_1$ - $\gamma$  caused thiol modulation of the enzyme (19, 20). In contrast, substitution of these two cysteines with serine in the  $\gamma$  subunit of  $CF_0CF_1$  from the green algae *Chlamydomonas reinhardtii* abolished the redox sensitivity (21).

In chloroplasts, many enzyme activities are regulated by thioredoxin (17, 22, 23). Although physiological significance of the redox regulation of these enzymes is still ambiguous, thioredoxin may play an important role to switch on a certain set of enzymes involved in the alternation of metabolisms in chloroplasts dependent on light and dark conditions. However, not very much is known regarding the molecular mechanism of redox regulation of the chloroplast enzymes so far. Because of the lack of the three-dimensional structure information of the regulatory region of  $CF_1$ - $\gamma$ , we still cannot determine the molecular mechanism of the regulation of  $CF_1$ .

In our previous study, we had introduced the regulatory region of the  $\gamma$  subunit of redox-sensitive  $CF_1$ -ATPase into the  $\gamma$  subunit of thermophilic bacterial  $F_1$ -ATPase and obtained the redox-sensitive chimeric complex (24). This complex was designated  $\alpha_3\beta_3\gamma_{TCT}$  complex. We then observed the real-time rotation behavior of this chimeric complex at a single molecule level (25). We succeeded in observing the regulation of rotation of the  $\gamma$  subunit of this chimeric complex by changing redox conditions under the microscope and revealed that the suppressed enzyme activity of the oxidized form complex was characterized by more frequent prolonged pauses during rotation of  $\gamma$ . Recently, a unique resting position of  $\gamma$  in the molecule of the oxidized form  $CF_0CF_1$  was proposed by electron microscopic analysis of the enzyme prepared from spinach leaves (26). Whether this apparent resting position has a relation with the prolonged pause of the rotation of  $\gamma$  is not known yet.

To understand the redox regulation of  $F_1$  thoroughly, we attempted the intimate analysis of the regulated rotation of  $\gamma$ . For the purpose, we compared the rotation behavior of two chimeric enzyme complex: the original chimeric complex containing the regulatory region of  $CF_1$ - $\gamma$ , which was designated TCT complex in this article, and the mutant chimeric complex whose three negatively charged residues at the regulatory region of  $CF_1$ - $\gamma$  were deleted. The latter complex was designated  $\Delta EDE$  complex here. We had already reported that this deletion of three negatively charged residues (Glu<sup>210</sup>-Asp<sup>211</sup>-Glu<sup>212</sup>) adjacent to the two cysteine residues caused inverse regulation of the enzyme activity in the chimeric complex, which was reconstituted from the  $\alpha$  and  $\beta$  subunits of bacterial  $F_1$ -ATPase and the  $\gamma$  subunit of spinach  $CF_1$  (27). Using this mutant complex containing the  $\Delta EDE$  mutation, we successfully observed an inverse redox regulation of the rotation behavior of the mutant  $\gamma$  subunit. A comparison of rotation behavior of TCT complex and that of  $\Delta EDE$  complex provides us the information on the authentic properties of redox regulation without undesirable effects of the reducing and oxidizing reagents for the observation setup for rotation.

#### EXPERIMENTAL PROCEDURES

**Materials**—Biotin-PEAC<sub>5</sub>-maleimide was purchased from Dojindo (Kumamoto, Japan). Carboxylated polystyrene beads were from Polysciences (Warrington, PA). Other chemicals were of the highest grade commercially available.

**Preparation of the Chimeric Complex**—The original  $\alpha_3\beta_3\gamma$  chimeric complex designated TCT was generated by the substitution of the central region of  $\gamma$  from thermophilic bacterial  $F_1$  with the counterpart of spinach chloroplast  $F_1$ - $\gamma$  as described previously (24). For an efficient biotin labeling, additional two cysteine residues were introduced into the position of Leu<sup>109</sup> and Ile<sup>249</sup> (the number is for the engineered  $\gamma$  subunit of the TCT-chimeric complex). In addition, we newly constructed the mutant complex ( $\Delta EDE$  complex) by deletion of three negatively charged residues Glu<sup>210</sup>-Asp<sup>211</sup>-Glu<sup>212</sup> in the regulatory region of the  $\gamma$  subunit in the TCT complex. Mutation was accomplished

by a quick-change method using appropriate primers (28). Both the TCT and  $\Delta EDE$  complexes were successfully expressed in *E. coli* strain JM103 AuncB-D, and the proteins were prepared as described previously (25) with slight modification. The chimeric complex was purified from the *E. coli* cell extract using a nickel-nitrilotriacetic acid Superflow column (Qiagen) and then applied to gel-filtration chromatography on a Superdex 200 column (16/30, Amersham Biosciences), which was equilibrated with 100 mM potassium phosphate, 100 mM KCl, and 1 mM EDTA, pH 7.0. The purified proteins were labeled with a 2-fold excess molar ratio of Biotin-PEAC<sub>5</sub>-maleimide for 1 h at room temperature, and then the excess reagents were removed by gel filtration on a NAP5 column (Amersham Biosciences), which was equilibrated with 10 mM MOPS-KOH and 50 mM KCl, pH 7.0. The TCT complex was reduced by 4  $\mu$ M thioredoxin-*f* and 200  $\mu$ M DTT prior to the following analysis as described previously (24). In contrast, the  $\Delta EDE$  complex did not require any pretreatments because it was spontaneously oxidized during the purification steps. The  $\Delta EDE$  complex then was fully activated.

**Rotation Assay**—To observe redox switching of rotation behavior of the  $\gamma$  subunit of the TCT and  $\Delta EDE$  complexes at a single molecule level, we employed the reduced form chloroplast thioredoxin-*f* as reductant as described previously (24, 29) and DTNB for oxidation instead of the low concentrations of CuCl<sub>2</sub> that we employed for our previous study (25). The appropriate concentrations of DTNB are reported to catalyze the formation of a disulfide bond by modification of the sulfidryl residues and the following rapid disulfide bond exchange (30).

To monitor the rotation, the  $\gamma$  subunits of the TCT and  $\Delta EDE$  complexes were labeled with polystyrene beads as follows. Polystyrene beads were biotinylated as described by Shimabukuro *et al.* (31). 15  $\mu$ l of the biotinylated complex (100–500 nM) in an assay mixture containing 10 mM MOPS-KOH, pH 7.0, 50 mM KCl, and 2 mM MgCl<sub>2</sub> supplemented with 1% (w/v) BSA was infused into a flow-chamber (8). After incubation for 2 min at room temperature, unattached complexes to the glass surface were washed out with 50  $\mu$ l of the assay mixture without BSA. 15  $\mu$ l of 5  $\mu$ M streptavidin dissolved in the assay mixture without BSA then was infused into the flow-chamber. After incubation for 2 min, excess streptavidin was washed out with 50  $\mu$ l of the assay mixture. The biotinylated polystyrene beads suspended in the assay mixture containing 1% (w/v) BSA were infused into the flow-chamber. After incubation for 30 min, unattached beads were washed out with 100  $\mu$ l of the assay mixture without BSA. Finally, rotation of the  $\gamma$  subunit of the complex was initiated by the addition of 100  $\mu$ l of the assay mixture with 2 mM ATP. Observation of rotation of the TCT complex was first carried out in the presence of 4  $\mu$ M thioredoxin-*f* and 200  $\mu$ M DTT for 5 min. 100  $\mu$ l of the assay mixture containing 250  $\mu$ M DTNB then was infused to oxidize the complex, and the observation was continued for another 5 min. To observe rotation of the  $\Delta EDE$  complex, the assay was first carried out without any oxidizing reagents because the enzyme was spontaneously oxidized during the purification steps as mentioned. 100  $\mu$ l of the assay mixture containing 4  $\mu$ M thioredoxin-*f* and 200  $\mu$ M DTT then was infused to reduce the complex, and the observation was continued for another 5 min. Rotation of the polystyrene beads attached to the  $\gamma$  subunit of both chimeric complex was observed with a conventional optical microscope type IX70 (Olympus, Tokyo, Japan) equipped with a CCD camera. The observed images were recorded to a digital video recorder and were analyzed with an image analysis software (8).

**Data Analysis**—To determine the frequency and the length of the pauses during rotation of the  $\gamma$  subunit, we analyzed the accumulated data as follows. Rotation of the  $\gamma$  subunit of the complex was recorded with the rate of 30 video frames/s. We calculated a displacement of the rotation from the first video frame to the third one, and then the obtained value (revolution per two frames) was plotted. Based on this definition, the displacement value should be 1.0 when the beads show full rotation (360°) within these three frames. Consequently, we defined a behavior of the beads whose displacement was <0.2 as a pause in this study. We then calculated the frequency and the length of the pauses and the rotation rate between the pauses with the original software. For the pause analysis, we used GruGruArrest and, for the rotation rate analysis, we used GruGruMawaru, respectively.

**ATPase Activity**—ATPase activity was measured at 25 °C in the presence of an ATP-regenerating system (32). The assay mixture containing 50 mM MOPS-KOH, pH 7.0, 100 mM KCl, 2 mM MgCl<sub>2</sub>, 2 mM ATP, 50  $\mu$ g/ml pyruvate kinase, 50  $\mu$ g/ml lactate dehydrogenase, 2 mM phosphoenolpyruvate, and 0.2 mM NADH was previously incubated at 25 °C. The reaction was then initiated by the addition of 5–10  $\mu$ g of the purified complex into 2 ml of the reaction mixture. The activity was measured by monitoring the decrease of absorption at 340 nm, and the activity of ATP hydrolysis in the steady state was determined.

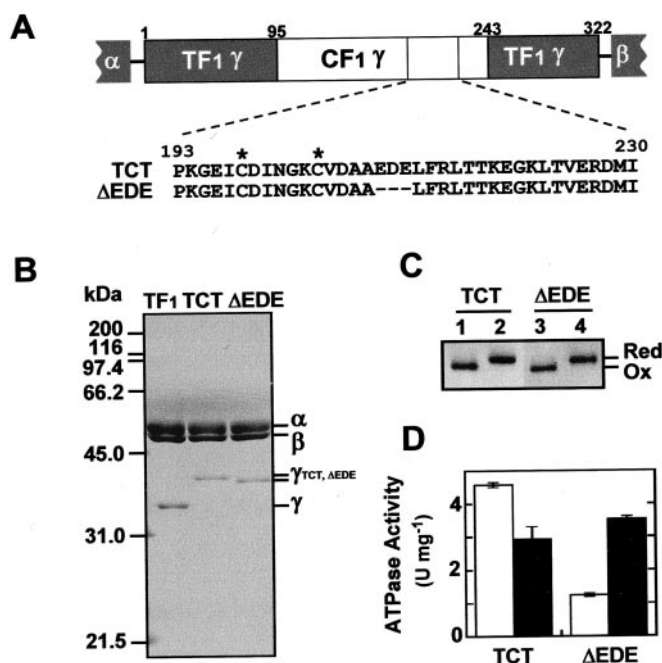


**FIG. 1. Reduction and oxidation of the TCT and  $\Delta$ EDE chimeric complexes.** A, the amino acid sequences of the introduced regulatory region into  $\gamma$  were shown. The  $\Delta$ EDE complex was generated by deletion of the three negatively charged residues close to two regulatory cysteine residues (indicated by asterisks) in the  $\gamma$  subunit of the TCT complex. B, 2  $\mu$ g of purified complexes were subjected to SDS-PAGE analysis, and the protein bands were visualized by Coomassie Brilliant Blue staining. C, the disulfide bond formation on the  $\gamma$  subunit of the both complexes was monitored by the AMS-labeling method as described under "Experimental Procedures." Purified proteins were oxidized in the presence of 100  $\mu$ M  $\text{CuCl}_2$  (lanes 1 and 3) or reduced with 4  $\mu$ M thioredoxin-*f* and 200  $\mu$ M DTT (lanes 2 and 4) prior to AMS-labeling, and labeled proteins were analyzed by SDS-PAGE. D, the ATPase activity was measured by an ATP-regenerating system. Purified TCT and  $\Delta$ EDE complexes were reduced with thioredoxin-*f* and DTT (open columns) or oxidized with  $\text{CuCl}_2$  (shaded columns) prior to the assay.

## RESULTS AND DISCUSSION

**Redox Regulation of Chimeric Enzymes**—In this study, we compared the redox regulation of two redox-sensitive chimeric complexes. Inverse redox regulation of ATPase activity by  $\Delta$ EDE mutation was first observed using the hybrid enzyme comprised of the  $\alpha$  and  $\beta$  subunits of thermophilic bacterial  $F_1$  and the recombinant chloroplast  $\gamma$  subunit (27). The obtained hybrid enzyme complex containing  $\Delta$ EDE mutation showed the higher ATPase activity when the regulatory cysteines were oxidized and less active when reduced. Here we introduced this mutation into the TCT complex (Fig. 1A). The desired complex,  $\Delta$ EDE complex, was expressed in *E. coli* (Fig. 1B). We then confirmed the formation and reduction of a disulfide bond on the regulatory region of both chimeric complexes by using AMS-labeling method (33) after biotin labeling the  $\gamma$  subunit via the two newly introduced cysteine residues (Cys<sup>109</sup> and Cys<sup>249</sup>) to attach polystyrene beads. When the TCT and  $\Delta$ EDE complexes were fully reduced by thioredoxin-*f* and DTT, the shifts of the protein bands corresponding to the  $\gamma$  subunit were observed (Fig. 1C).

As expected, the ATPase activity of the  $\Delta$ EDE complex under oxidizing conditions was attenuated to 34% of that under reducing conditions (Fig. 1D), whereas the activity of the TCT complex under reducing conditions was stimulated up to 1.6-fold of that of the oxidized one. The ATPase activity of the oxidized  $\Delta$ EDE complex was slightly lower than that of the reduced TCT complex, and this result was somewhat different

from our previous results obtained by using the hybrid enzyme complex reconstituted from TF<sub>1</sub>- $\alpha$  and  $\beta$  subunits and the CF<sub>1</sub>- $\gamma$  subunit (27). However, from the comparison of these ATPase activities, we cannot conclude whether the oxidized form  $\Delta$ EDE complex mimics the reduced form TCT complex or the oxidized form complex.

**Redox Regulation of Rotation**—To monitor the rotation behavior of the  $\gamma$  subunit, we adopted the polystyrene beads instead of the fluorescent-labeled actin filaments. This allowed us to observe the rotation of  $\gamma$  with the conventional microscope even under oxidizing conditions as described previously (25). We first observed the rotation behavior of the reduced form TCT complex for 5 min and then gently exchanged the buffer in the chamber to the buffer for oxidation. We then observed the behavior of the beads for another 5 min.

As shown in Fig. 2A, the beads attached to the TCT complex rotated continuously with the brief pauses under reducing conditions. When oxidized, the beads stopped frequently during rotation and the long pauses emerged. These results were consistent with those of our previous study (25). In contrast, the beads attached to the  $\Delta$ EDE complex rotated smoothly under oxidizing conditions (Fig. 2B). After switching to reducing conditions, they stopped frequently. This way we successfully observed inverse regulation of rotation of the  $\Delta$ EDE complex by switching the redox conditions. The observed redox switching of rotation behavior of the  $\Delta$ EDE complex was apparently paralleled to that of the TCT complex with the exception of alternating the oxidized state with the reduced state. These results strongly suggest that the long and frequent pauses, which were observed on the rotation of the oxidized form TCT complex or that of the reduced form  $\Delta$ EDE complex, should be caused by the suppressed state of each of the complexes but not by either oxidizing or reducing conditions themselves. In other words, these results exclude the possibility that oxidizing or reducing conditions induced the special interaction between, for example, beads and glass surface, which may affect the rotation behavior of the enzyme.

When we observed the rotation behavior of the both complexes, we noticed that a couple of the beads showed occasional stops after the buffer exchange (Fig. 2, C and D), although the frequency of the pauses caused by this buffer exchange was less evident than that caused by the redox switching. As we found that some of the TF<sub>1</sub> complex stopped occasionally after the buffer exchange (data not shown), we concluded that the pauses resulting from buffer exchange were not peculiar to the TCT and  $\Delta$ EDE complexes. The buffer exchange might induce collision of the beads with steric obstacles on the glass surface.

**Frequency of the Pauses during Rotation**—We next determined the length and the frequency of pauses and the rotation rates of both complexes. Because the original rotation data contained both enzyme movement and Brownian motion of the beads, we calculated the displacement of the beads image from the first video frame to the third one and plotted it (Fig. 2E). In this study, we defined a period whose displacement value was under 0.2 during a three-frame observation as a pausing period, which was shown as black bar on the upper part of Fig. 2E. Based on this definition, we calculated the length and the frequency of the pauses during the whole observation period. Even when we put the enzymes to the suppressed states, they did rotate and did not stop completely over the whole periods. These allowed us to calculate the rotation rate under all of the experimental conditions.

The proportion of the pauses during the observation period was calculated for each of the complexes under reduced or oxidized conditions (Fig. 2F). Although a slight increase in the proportion of the pauses was observed only by the buffer ex-

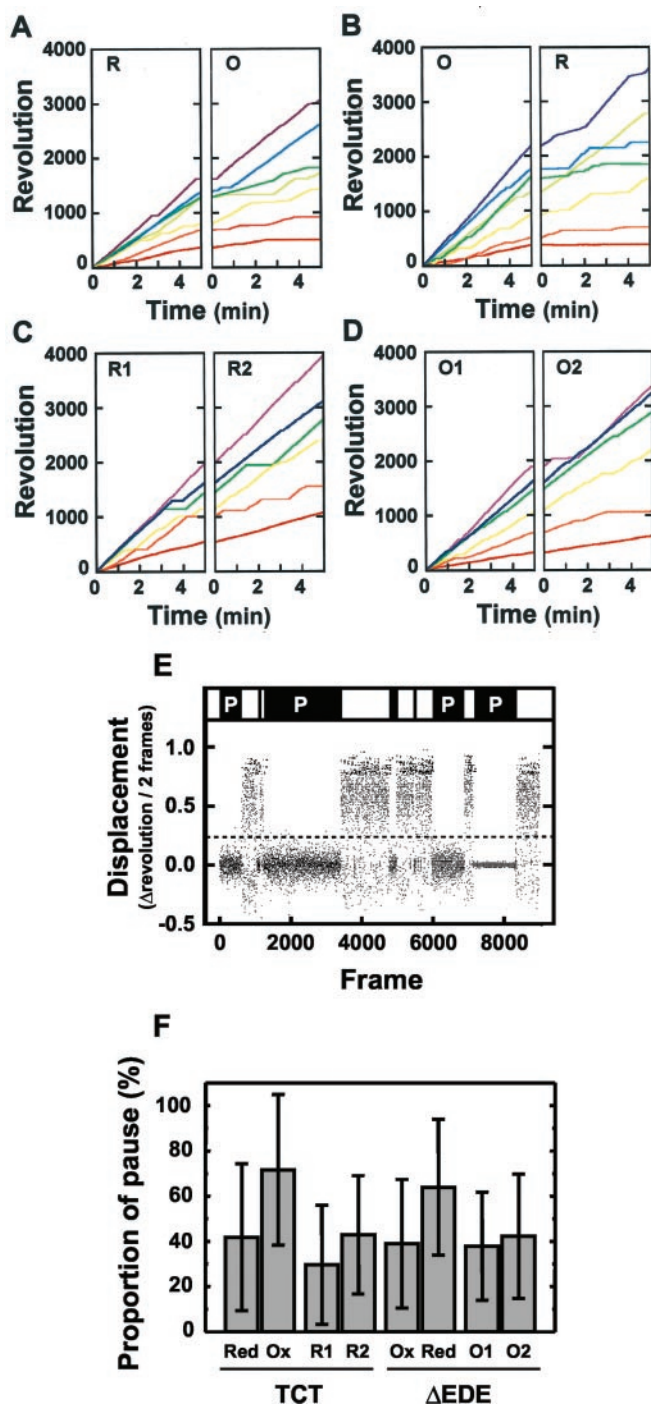


**FIG. 2. The rotation of the  $\gamma$  subunit in the TCT and  $\Delta$ EDE chimeric complexes.** A–D, polystyrene beads (diameter 0.35  $\mu$ m) were attached to the  $\gamma$  subunit of the TCT (A and C) and  $\Delta$ EDE (B and D) complex, and rotation of the beads was observed. Rotation of the  $\gamma$  subunit of TCT complex was observed under reducing conditions for 5 min (R), and after switching to oxidizing conditions by buffer exchange, observation was further continued for 5 min (O). In contrast, rotation the  $\gamma$  subunit of  $\Delta$ EDE was observed under oxidizing conditions (O), and after switching to reducing conditions by buffer exchange, observation was further continued (R). The effects of the buffer exchange were assessed for both complexes (C and D). In each case, it took <1 min to exchange buffer in the flow-chamber. Each of the traces shows the anti-clockwise rotation of the beads. The total number of particles observed is as follows: 18 for A; 32 for B; 28 for C; and 43 for D, respectively. E, the movement of the beads during rotation was analyzed by image analysis software CREST Image, and the displacement of the beads within three frames was plotted. The rotation was recorded by the rate of 30 video frames/s. As an example, the displacement data calculated from rotation of the oxidized TCT complex are shown. A phase where the displacement value was <0.2 was defined as a pause. F, proportion of the pauses during rotation of each of the complexes under the different redox conditions were calculated based on the pause analysis method described above using all of the data of the rotating beads observed in this study.

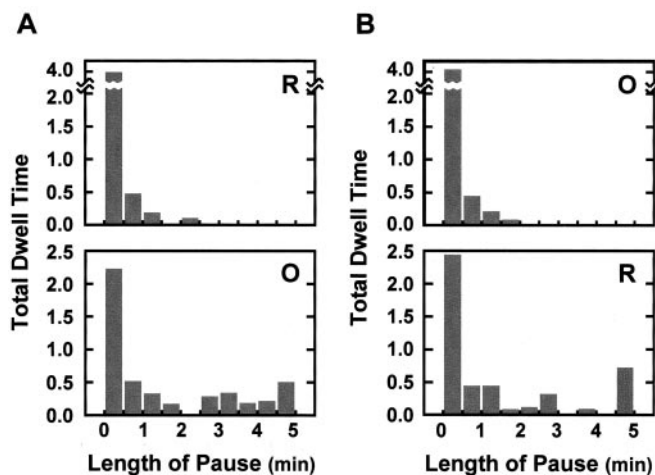


**FIG. 3. Frequency of the pauses during rotation.** A, the frequency and length of pauses during rotation of the  $\gamma$  subunit of the TCT complex was determined from the data observed under reduced (R) and oxidized (O) conditions. The number of pauses for each length was counted. The vertical axis shows the total dwell time of the beads calculated from (the number of the events)  $\times$  (the length of the pause). B, the frequency and length of pauses during rotation of the  $\gamma$  subunit of the  $\Delta$ EDE complex was determined as for the TCT complex.

change for TCT from R1 phase to R2 phase and for  $\Delta$ EDE from O1 phase to O<sub>2</sub> phase, the pause ratios were remarkably increased when the TCT complex was oxidized or when the  $\Delta$ EDE complex was reduced.

In case of the TCT complex, the frequency of the pause longer than 2 min certainly increased especially under oxidizing conditions (Fig. 3A). On the contrary, the frequency of the long pause of the  $\Delta$ EDE complex increased under reducing conditions (Fig. 3B). A great deal of interest was focused on whether the suppressed chimeric complex took a certain position for pause or not. However, we could not settle this question in this study because the pauses observed in our experiments contained a lot of short pauses, which are also observed even under the active state conditions. With regard to the position of the pause, a unique resting position of the oxidized  $CF_0CF_1$  was recently suggested by electron microscope analysis of the ATPase complex prepared from spinach leaves (26). We cannot directly adopt the reported resting position to the pause position during rotation because their resting position was simply characterized by orientation of the  $\gamma$  subunit and position of the stator, which was formed by subunits  $\delta$ , I, II, and IV. In our case, the observed pause positions must contain three different types: the pause induced by the redox regulation, the pause induced by the buffer exchange, and the pause of ADP-inhibition as mentioned below.

$F_1$ -ATPase occasionally falls into the ADP-inhibited state in the presence of submicromolar ATP (32). From the intimate analysis of the rotation of  $F_1$ -ATPase, Hirono-Hara *et al.* (34) recently reported that the ADP-inhibited states cause the pauses with a lifetime of 1.7 s and the other pauses with a lifetime of 32 s at the concentration of 2 mM ATP (34). The enzyme trapped in this inhibition state can be easily recovered, and the rotation is re-started when the assay mixture contains high concentrations of ATP. Brief pauses observed in our experiments may be attributed to the ADP-inhibited states of the enzyme as reported previously (34). When we calculated the

Based on this definition, the length and the number of pause were calculated. F, proportion of the pauses during rotation of each of the complexes under the different redox conditions were calculated based on the pause analysis method described above using all of the data of the rotating beads observed in this study.

TABLE I  
Rotation rates of TCT and  $\Delta$ EDE complexes

Based on the definition of pause shown in Fig. 2E, a phase with the exception of the pause was regarded as rotating phase and the rotation rates for each phase were calculated. Median and mean values are shown.

	Redox state	Rotation rate	
		Median	Average
		<i>revolution s<sup>-1</sup></i>	
TCT	R	3.17	3.46 ± 1.29
	O	3.16	3.28 ± 1.59
	R1	3.76	4.09 ± 1.37
	R2	3.66	4.10 ± 1.59
$\Delta$ EDE	O	3.35	3.66 ± 1.11
	R	3.39	3.79 ± 1.31
	O1	3.53	3.89 ± 1.40
	O2	3.38	3.77 ± 1.50

proportion of the pause period during our observation, we found that 30–40% of the pauses were observed under all of the experimental conditions (Fig. 2F). These basal values must be due to the ADP inhibition state. Thus, we mainly focused on the pauses longer than 2 min in this study.

**Rates of Rotation under the Regulated Conditions**—As mentioned above, the suppression of the ATPase activity in both the TCT and  $\Delta$ EDE complexes by the conformational change of the regulatory region should be mainly attributable to long and more frequent pauses. To confirm this assumption, we here analyzed the rotation rates of the beads (Table I). The rotating stage was defined as the period where the beads do not show the pauses based on the definition shown in Fig. 2E. The TCT and  $\Delta$ EDE complexes showed no remarkable differences in the rotation rates under either the reduced states or the oxidized states. The buffer exchange also had no effect on the rotation rates of the TCT and  $\Delta$ EDE complexes.

These results gave us a clue to determine the mechanism of redox regulation of ATPase. Formation of the disulfide bond on the regulatory region of the  $\gamma$  subunit must induce a conformational change of this subunit. Because we still do not have any information on the structure of the regulatory region of  $CF_1$ - $\gamma$ , it is impossible to presume the resultant structure now after this conformational change. However, we can speculate that the conformational change induced by the formation or reduction of this disulfide bond on  $\gamma$  will induce a certain situation, which will disturb the smooth rotation of the  $\gamma$  subunit in the complex. From the torque calculation on the rotation of  $\gamma$  (8), the rotation promoted by ATP hydrolysis is enough strong to break the hydrogen bonds between the  $\gamma$  subunit and the surrounding  $\alpha$  and  $\beta$  subunits. In addition, the observed rotation rate itself is significantly decreased by the attached prove, which is huge in comparison to the size of the enzyme molecule. Therefore, the rate-limiting of rotation of the beads must be mainly determined by the size of the beads itself. From this point of view, it is conceivable that the rotation rate of the  $\gamma$  subunit is not affected directly by formation or reduction of the disulfide bridge on  $\gamma$ .

Finally, we calculated the averaged rotation rates for 5 min of observation under reducing or oxidizing conditions and compared the values with those for ATPase activity (Fig. 1D and Table II). The averaged rotation rate of the oxidized TCT complex was suppressed to 43% of that of the reduced state. In contrast, the rate of the rotation of the reduced  $\Delta$ EDE complex was suppressed to 57% of the rate of the oxidized state. The ATPase activity of the oxidized TCT complex was 64% of the reduced state, and that of the reduced  $\Delta$ EDE complex was 34% of the oxidized state, respectively (Fig. 1D). Hence, the responses of the averaged rotation rates of both the TCT and

TABLE II  
Averaged rates of the rotation of the TCT and  $\Delta$ EDE complexes

The rates of rotation including pausing periods were calculated as averaged rates of rotation. The relative values of the average rates of rotation after the buffer exchange were shown in the right column.

	Redox state	Rotation rate (average)	
		<i>revolution s<sup>-1</sup></i>	%
TCT	R	3.20 ± 1.47	
	O	1.36 ± 1.45	42.5
	R1	4.00 ± 1.51	79.3
	R2	3.17 ± 1.82	
$\Delta$ EDE	O	3.57 ± 1.95	
	R	2.05 ± 1.79	57.3
	O1	3.47 ± 1.30	
	O2	3.27 ± 1.67	94.3

$\Delta$ EDE complexes to the redox switching were roughly consistent with those of ATPase activity of these complexes. Therefore, we conclude that the suppressed enzyme activity of the chimeric complex under either oxidizing or reducing conditions was mainly due to long and frequent pauses during rotation, irrespective of the rotation rate between the pauses.

**Conclusion**—Redox regulation of the enzyme activity of both TCT and  $\Delta$ EDE complexes by redox switching is not like an all-or-none way. Therefore, it is very important to observe the rotation behavior of the single molecule enzyme and its regulation to understand the redox regulation of  $F_1$ -ATPase at the molecular level. In this study, the  $\Delta$ EDE complex was a good reference for the observation of the redox regulation of rotation by the regulatory region of chloroplast  $F_1$ -ATPase. This approach made it possible to compare the pause and the rotation behavior of the single molecule  $F_1$  under suppressed and stimulated conditions rather than simple reduced and oxidized conditions. Consequently, we could reveal that the suppression of the enzyme activity by the regulatory region derived from  $CF_1$ - $\gamma$  should reflect the long and frequent pauses of rotation but not the change of the rotation rate itself. How the conformational change of the regulatory region can control the frequency of the pause during rotation must be clarified by the structural background in future.

**Acknowledgments**—We thank Fumie Koyama for technical assistance and Katsuya Shimabukuro and Takayuki Ariga for their technical advice. Special thanks to Prof. Masasuke Yoshida and Prof. Heinrich Strotmann for their valuable suggestions.

#### REFERENCES

- Boyer, P. D. (1997) *Annu. Rev. Biochem.* **66**, 717–749
- Senior, A. E. (1990) *Annu. Rev. Biophys. Biophys. Chem.* **19**, 7–41
- Yoshida, M., Muneyuki, E., and Hisabori, T. (2001) *Nat. Rev. Mol. Cell. Biol.* **2**, 669–677
- Yoshida, M., Sone, N., Hirata, H., Kagawa, Y., and Ui, N. (1979) *J. Biol. Chem.* **254**, 9525–9533
- Matsui, T., Muneyuki, E., Honda, M., Allison, W. S., Dou, C., and Yoshida, M. (1997) *J. Biol. Chem.* **272**, 8215–8221
- Abrahams, J. P., Leslie, A. G., Lutter, R., and Walker, J. E. (1994) *Nature* **370**, 621–628
- Gresser, M. J., Myers, J. A., and Boyer, P. D. (1982) *J. Biol. Chem.* **257**, 12030–12038
- Noji, H., Yasuda, R., Yoshida, M., and Kinosita, K., Jr. (1997) *Nature* **386**, 299–302
- Noji, H., Hasler, K., Junge, W., Kinosita, K., Jr., Yoshida, M., and Engelbrecht, S. (1999) *Biochem. Biophys. Res. Commun.* **260**, 597–599
- Omote, H., Sambonmatsu, N., Saito, K., Sambongi, Y., Iwamoto-Kihara, A., Yanagida, T., Wada, Y., and Futai, M. (1999) *Proc. Natl. Acad. Sci. U. S. A.* **96**, 7780–7784
- Hisabori, T., Kondoh, A., and Yoshida, M. (1999) *FEBS Lett.* **463**, 35–38
- Groth, G., and Pohl, E. (2001) *J. Biol. Chem.* **276**, 1345–1352
- Junesch, U., and Gräber, P. (1987) *Biochim. Biophys. Acta* **893**, 275–288
- Bunney, T. D., van Walraven, H. S., and de Boer, A. H. (2001) *Proc. Natl. Acad. Sci. U. S. A.* **98**, 4249–4254
- Mills, J. D., Mitchell, P., and Schürmann, P. (1980) *FEBS Lett.* **112**, 173–177
- Nalin, C. M., and McCarty, R. E. (1984) *J. Biol. Chem.* **259**, 7275–7280
- Jacquot, J. P., Rouhier, N., and Gelhaye, E. (2002) *Ann. N. Y. Acad. Sci.* **973**, 508–519
- Miki, J., Maeda, M., Mukohata, Y., and Futai, M. (1988) *FEBS Lett.* **232**, 221–226

19. Werner-Grüne, S., Gunkel, D., Schumann, J., and Strotmann, H. (1994) *Mol. Gen. Genet.* **244**, 144–150
20. Krenn, B. E., Strotmann, H., Van Walraven, H. S., Scholts, M. J., and Kraayenhof, R. (1997) *Biochem. J.* **323**, 841–845
21. Ross, S. A., Zhang, M. X., and Selman, B. R. (1995) *J. Biol. Chem.* **270**, 9813–9818
22. Motohashi, K., Kondoh, A., Stumpp, M. T., and Hisabori, T. (2001) *Proc. Natl. Acad. Sci. U. S. A.* **98**, 11224–11229
23. Balmer, Y., Koller, A., del Val, G., Manieri, W., Schürmann, P., and Buchanan, B. B. (2003) *Proc. Natl. Acad. Sci. U. S. A.* **100**, 370–375
24. Bald, D., Noji, H., Stumpp, M. T., Yoshida, M., and Hisabori, T. (2000) *J. Biol. Chem.* **275**, 12757–12762
25. Bald, D., Noji, H., Yoshida, M., Hirono-Hara, Y., and Hisabori, T. (2001) *J. Biol. Chem.* **276**, 39505–39507
26. Mellwig, C., and Botzcher, B. (2003) *J. Biol. Chem.* **278**, 18544–18549
27. Konno, H., Yodogawa, M., Stumpp, M. T., Kroth, P., Strotmann, H., Motohashi, K., Amano, T., and Hisabori, T. (2000) *Biochem. J.* **352**, 783–788
28. Kirsch, R. D., and Joly, E. (1998) *Nucleic Acids Res.* **26**, 1848–1850
29. Stumpp, M. T., Motohashi, K., and Hisabori, T. (1999) *Biochem. J.* **341**, 157–163
30. Bulygin, V. V., Duncan, T. M., and Cross, R. L. (1998) *J. Biol. Chem.* **273**, 31765–31769
31. Shimabukuro, K., Yasuda, R., Muneyuki, E., Hara, K. Y., Kinoshita, K., Jr., and Yoshida, M. (2003) *Proc. Natl. Acad. Sci. U. S. A.* **100**, 14731–14736
32. Vasilyeva, E. A., Minkov, I. B., Fitin, A. F., and Vinogradov, A. D. (1982) *Biochem. J.* **202**, 9–14
33. Kobayashi, T., Kishigami, S., Sone, M., Inokuchi, H., Mogi, T., and Ito, K. (1997) *Proc. Natl. Acad. Sci. U. S. A.* **94**, 11857–11862
34. Hirono-Hara, Y., Noji, H., Nishiura, M., Muneyuki, E., Hara, K. Y., Yasuda, R., Kinoshita, K., Jr., and Yoshida, M. (2001) *Proc. Natl. Acad. Sci. U. S. A.* **98**, 13649–13654